Development of new Mn-based oxygen carriers using MgO and SiO<inf>2</inf> as supports for Chemical Looping with Oxygen

Fuel 337 (2023) 127177

Contents lists available at ScienceDirect

Fuel

journal homepage: www.elsevier.com/locate/fuel

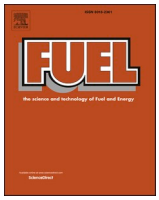

Full Length Article

Development of new Mn-based oxygen carriers using MgO and SiO_2 as supports for Chemical Looping with Oxygen Uncoupling (CLOU)

Iñaki Adánez-Rubio [a,*], Tobias Mattisson [b], Marijke Jacobs [c], Juan Adánez [a]

[a] Instituto de Carboquímica (ICB-CSIC), Department of Energy & Environment, Miguel Luesma Castán, 4, Zaragoza 50018, Spain
[b] Department of Energy and Environment, Division of Energy Technology, Chalmers University of Technology, SE-412 96 Göteborg, Sweden
[c] Unit Sustainable Materials Management, Flemish Institute for Technological Research (VITO), Boeretang 200, Mol 2400, Belgium

ARTICLE INFO

Keywords:
CO_2 capture
CLOU
Manganese
Magnesium
Silicon

ABSTRACT

Chemical Looping with Oxygen Uncoupling (CLOU) is a technological adaptation of CLC, most applicable for the combustion of solid fuels. In the CLOU process, an oxygen carrier in the fuel reactor, avoiding the direct contact of the fuel with the air, releases the oxygen needed for the fuel combustion. The oxygen carrier is regenerated with air in the interconnected air reactor. The present work explores the behavior of the system Mn/Mg/Si as oxygen carriers for chemical-looping with oxygen uncoupling (CLOU). Six different mixed oxides of the system Mn/Mg/Si were investigated for the CLC/CLOU process. Materials were prepared by spray drying with different metal ratios used in the investigation. The properties of interest for the viability of these materials are the lattice oxygen supply for CLC and the gaseous oxygen release for CLOU, properties that were explored in a TGA. Further, the fluidization behavior and the mechanical resistance were investigated in a batch fluidized bed reactor. In the TGA it was observed that the most reactive oxygen carriers for the CLOU process were materials without Si in the structure, more specifically M24Mg76 and M48Mg51 which had a molar ratio of Mn/Mg of 0.17 and 0.51 respectively. It was also observed that for the oxygen carriers with Si in the composition, the regeneration was very poor. Oxygen carriers M24Mg76 and M48Mg51 were selected for batch fluidized bed reactor testing showing good behavior with respect to the CLOU reactivity, and mechanical stability. One of the materials, the M24Mg76 showed activation during the experiments in the batch fluidized bed reactor experiments, increasing the oxygen transport capacity by 20 % during the experiment. However, 10 vol% of O_2 was needed to regenerate both oxygen carriers at 850 °C. No agglomeration tendencies were seen, and the attrition rate was low, obtaining high-extrapolated lifetime values. The fact that highly reactive oxygen carriers can be made with cheap and highly available metals oxides, i.e. Mn and Mg, makes this system very promising and a possible alternative to benchmark Cu-based CLOU materials.

1. Introduction

Chemical Looping Combustion (CLC) is a combustion technology with inherent CO_2 separation and capture, characterized by very low energy penalty in comparison to other CO_2 capture technologies [1]. In the CLC process the oxygen needed for the fuel combustion is supplied by an oxygen carrier in the fuel reactor (FR), usually a metal oxide (Me_xO_y), avoiding the direct contact of the fuel with the air. The metal oxide is reduced in the FR to Me_xO_{y-1}, and regenerated with air in the interconnected air reactor (AR). The enthalpy regarding both reactors is the same as in conventional combustion, thus CLC has not inherent energy penalty. After water condensation a highly concentrated CO_2 stream is ready for storage. Due to its inherent CO_2 capture, CLC technology is promising for using in power plants with very low energy penalty.

Chemical Looping with Oxygen Uncoupling (CLOU) process is a technological adaptation of CLC very useful for the combustion of solids. This is mainly due to the characteristic of the oxygen carrier, which will release oxygen to the gas phase in the fuel reactor. Hence, solid fuel is converted by normal combustion in the fuel reactor, which is different for normal CLC, where the char is gasified with H_2O, CO_2 to syngas, which can react with the oxygen carrier particles in the same bed. Fig. 1 shows the CLOU process for solid fuels. The diagram includes a carbon stripper in order to recirculate the unburnt char to the fuel reactor.

* Corresponding author.
E-mail address: iadanez@icb.csic.es (I. Adánez-Rubio).

https://doi.org/10.1016/j.fuel.2022.127177
Received 9 October 2022; Received in revised form 6 December 2022; Accepted 13 December 2022
Available online 22 December 2022

The oxygen carrier behaviour with respect to the reactivity and attrition resistance are the key points of the CLOU technology. For CLC combustion by the CLOU mechanism CuO and Mn_2O_3 based oxygen carriers [2–5], mixed oxides as Cu-Mn [6–8], Cu-Mn-Fe magnetic materials [9,10] and calcium manganites with perovskite structure [11–13] have been proposed and tested. Mixed oxides containing Fe, Mn, Mg, Ca, Ti have also been used as oxygen carriers for solid fuel combustion supplying lattice oxygen [14–19]. Reviews focusing on CLC and CLC with solid fuels can be found elsewhere [20,21].

As oxygen carriers in the CLOU process, metal oxides need to release oxygen at high temperatures and can be regenerated also at high temperatures in the air reactor. Copper, manganese and cobalt oxides have been identified as active metal oxides [22,23]. Mn based mixed oxides with perovskite structure, mainly $CaMnO_3$ doped with Mg, Ti, release some gaseous oxygen and also supply lattice oxygen. These materials showed a good performance [24,25] for gaseous fuel combustion [26] although for solid fuel combustion the oxygen released was not sufficient to reach complete combustion to CO_2 and H_2O [14–17].

Materials utilizing Mn/Mg mixed oxides have been investigated in different applications, and could be of interest due to high availability and low cost. The phases of the system Mn/Mg were previously investigated to make refractory materials [27], oxygen sensors [28] and as oxygen carrier for CLC [29]. In these studies it was found that the main oxidized phases are Mg_6MnO_8, Mg_2MnO_4 and $MgMn_2O_4$. At low oxygen partial pressures the solid solution ($Mg_{1-x}Mn_x$) O disaggregated, $MgMn_2O_4$ and MgO are formed, releasing oxygen in a reversible way [28]. In the last years the mixed oxides of Mn-Mg and Mn-Si has been studied for their use as oxygen carriers for CLOU process [14–19,29–31].

Shulman et al. studied different mixed oxides with as Mn-Fe, Mn-Ni, Mn-Si [17] and Mn-Mg [29]. They observed that all the oxygen carriers showed oxygen release in CLOU conditions, and all the materials showed good CH_4 combustion behavior. However, these materials were not easy to regenerate, even Mn-Si materials cannot be re-oxidized with 10 vol% of O_2 [17]. Ryden et al. made a review about combined oxides as oxygen carriers, and they found that Mn-Si oxygen carriers has a great potential due to the high capacity to transport O_2 and low price. With respect to Mn-Mg materials they conclude that it is necessary to increase the research in this type of materials [31]. Frick et al. synthetized several oxygen carriers adding Mg, Al, Ti or Ca to Mn-Si oxygen carrier, and the material with Mg was the oxygen carrier with the best oxygen release for all the materials studied [14]. Mattisson et al. also studied the binary and tertiary Mn-based oxygen carriers. They found that the binary mixed oxides have good reactivity and oxygen release, overall Mn-Mg mixed oxides [18].

The aim of this work is to explore the behavior of the system Mn/Mg/Si as oxygen carriers for chemical-looping with oxygen uncoupling (CLOU). Materials were prepared by spray drying with different metal ratios. The properties of interest regarding lattice oxygen supply for CLC or gaseous oxygen for CLOU, together with the fluidization behavior and the mechanical resistance, were investigated and discussed. A series of materials including Si in the matrix were formulated in the study. The Mn-Si system has previously shown promise, [18], and hence it was decided to prepare a number of pseudo ternary materials of Mn-Mg-Si-O.

2. Experimental section

2.1. Materials

Oxygen carriers with different Mn/Mg/Si ratios were prepared by VITO by mechanical mixing of powders followed by spray drying and further calcined at different temperatures. The spray drying process was similar to the process described in previous work [32]. Mn_3O_4 from Chemalloy, MgO from Magchem 30 and SiO_2 from Silverbond M800 powder were used. Table 1 shows the composition of the six oxygen carriers prepared together with the calcination conditions used. Particles were sieved to a particle size +100–200 μm for fluidization experiments. The materials calcined a 1200 °C showed the better characteristics related to the relation temperature/crushing strength. Only the particles of M56Mg44 showed a significant increase of the crushing strength at higher temperature (1300 °C). For this reason, the oxygen carriers calcined at 1200 °C were selected to study in the present work.

2.2. Oxygen carrier characterization

Chemical and physical characteristics of the oxygen carriers were determined by different methods. Crushing strength and attrition jet index test were also used in order to gauge mechanical properties of the particles. Oxygen transport capacity for CLC (R_{OC}) was determined through the weight loss obtained by TGA during the reduction with H_2 at 800 °C, while the oxygen transport capacity for CLOU (R_{CLOU}) was measured in N_2 atmosphere at 950 °C in the TGA. Table 2 shows the main properties useful for Chemical Looping determined for the oxygen carrier particles.

The crushing strength of the particles was determined in a Shimpo FGN-5X crushing strength apparatus, and results are given as an average value of 20 measurements, with particles sized +0.1–0.3 mm. A three-hole air jet attrition equipment ATTRI-AS (Ma. Tec. Materials Technologies Snc) configured according to the ASTM-D-5757 standard [33] was used to determine the attrition resistance at low temperature. The Attrition Jet Index (AJI) was calculated considering the weight of fine particles recovered in the filter after 5 h of testing by the following equation.

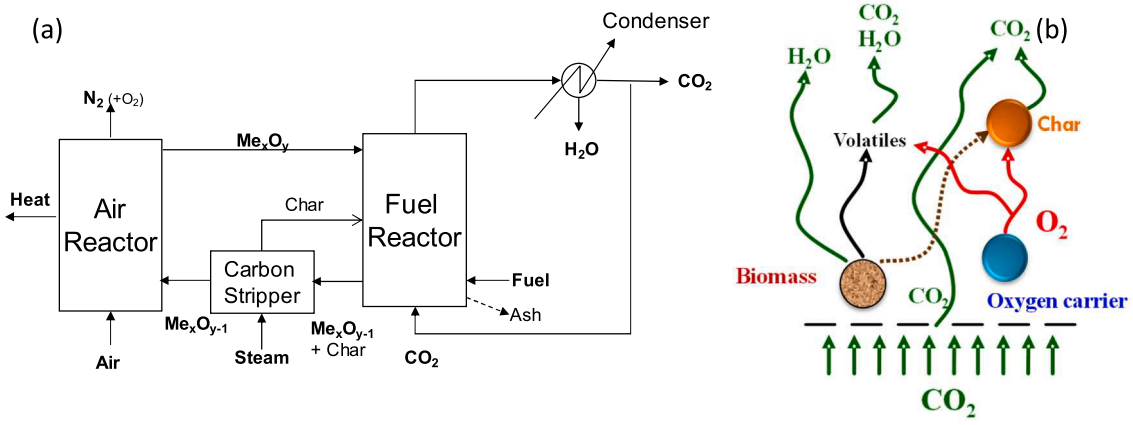

Fig. 1. (a) CLOU unit scheme for solid fuel and (b) Scheme of the CLOU process for solid fuel combustion.

Table 1
Oxygen carrier particles composition.

Mn/Mg						Mg/Mn/Si					
Number	Sample	Mg/Mn	Si/Mn	Calcination temp.	Crushing strength (N)	Number	Sample	Mg/Mn	Si/Mn	Calcination temp.	Crushing strength (N)
1	M56Mg44	1.6	0.0	1100	0.4	4	M61MgS12	0.8	0.2	1100	0.3
				1200	1.2					1150	0.4
				1300	2.3					1200	0.4
2	M48Mg51	2.0	0.0	1100	1.9	5	M56MgS7	1.2	0.2	1100	0.3
				1200	2.8					1150	0.3
				1300	2.3					1200	0.3
3	M24Mg76	6.0	0.0	1100	0.5	6	M53MgS4	1.5	0.1	1100	0.3
				1200	1.2					1150	0.3
				1300	1.8					1200	0.4

Table 2
Properties of the oxygen carrier particles.

Oxygen carrier	Crushing Strength (N)	$R_{0,CLC}$ (%)[a]	$R_{0,CLOU}$ (%)[b]	$r_{H_2} \bullet 10^3 (kgO/s \bullet kgOC)^a$	$r_{CH_4} \bullet 10^3 (kgO/s \bullet kgOC)^a$	$r_{O_2} \bullet 10^3 (kgO/s \bullet kgOC)^b$
M24Mg76_1200	1.2	5.3	2.0	2.9	0.6	0.1
M48Mg51_1200	1.9	8.7	2.3	3.5	0.7	0.1
M56Mg44_1200	1.2	9.5	2.5	3.1	0.9	0.1
M53MgS4_1200	0.3	8.8	2.2	3.1	0.6	0.1
M56MgS7_1200	0.3	8.3	2.6	3.5	0.5	0.1
M61MgS12_1200	0.3	6.9	0.2	3.1	0.3	0.0

[a] At 800 °C in the TGA.
[b] At 950 °C in the TGA.

$$\text{AJI} = \frac{m_{5h}}{m_s} \quad (1)$$

where m_{5h} is the mass collected of fines after 5 h from the attrition tester, and m_s is the mass of sample loaded into the system (nominally 50 g) [34]. It is apparent that incorporation of Si has a detrimental effect with respect to the mechanical properties, as the crushing strength of materials containing Si was lower than 1 N, independent of the calcination temperature.

The identification of crystalline chemical species was carried out by X-ray diffraction (XRD) spectra collected by a Bruker D8 Advance X-ray powder diffractometer equipped with an X-ray source with a Cu anode working at 40 kV and 40 mA and an energy-dispersive one-dimensional detector. The diffraction pattern was obtained over the 2θ range of 10° to 80° with a step of 0.019°. The oxygen carrier particles were also analyzed by scanning electron microscopy (SEM) using an SEM-EDX Hitachi S-3400 N with analyzer EDX Röntec XFlash de Si(Li).

All the tests on fresh oxygen carriers were performed before any TGA operations, whereas tests on used oxygen carriers, including the selected candidates the tests, were performed after batch fluidized bed reactor operation.

2.3. Experimental installations

2.3.1. Thermogravimetric analysis (TGA)

To determine the oxygen transport capacity of the oxygen carrier both for CLC and CLOU and also its reactivity, multiple isothermal redox cycles using 50 mg samples of oxygen carrier were carried out in a TGA, CI Electronics type, previously described elsewhere [35]. TGA reactivity of the oxygen carrier for CLC was measured by means of multiple redox cycles at isothermal conditions, and data measured in the third cycle were taken for fresh and used particles in order to calculate the CLC and CLOU reactivity values. Evolution change of the weight with time was measured during the reduction in 15 % CH_4 and 20 % H_2O in order to analyze the oxygen carrier reactivity. The oxidation was made in air. The $R_{0,CLC}$ as the total oxygen transport capacity of an oxygen carrier was calculated in the third reduction cycle with 15 % H_2 and 20 % H_2O and oxidation in air at a temperature of 800 °C. CLOU reactivity was measured in N_2 atmosphere during third reduction redox cycle in N_2/air at temperatures from 800 to 950 °C. The $R_{0,CLOU}$ as the CLOU oxygen transport capacity of an oxygen carrier was calculated in the third reduction with N_2 cycle at 950 °C. All the TGA experiments were carried out in conditions under chemical reaction control as described in [35].

Thermal cycling experiments were made in the TGA. The aim of these experiments was to determine at what temperature the materials absorb and release oxygen, as this was not known prior to this work. In these experiments, the oxygen carrier was heated in 10 vol% O_2 up to 950 °C. Afterwards the temperature was decreased in 25 °C steps down to 800° C. In each step sample was weighted until stabilization or during 30 min. When reaching 800 °C there should be no reaction with oxygen at stable conditions, and once this temperature was reached, the temperature was increased in steps from 25 °C to 1025 °C. The oxygen concentration was maintained at 10 vol% throughout the temperature swing cycles. In these steps, the temperature at which the oxygen carrier is able to release oxygen (reduce) to the atmosphere around the particles was determined.

Once the sample weight was stable at the maximum temperature, it was decreased to 800 °C in steps of 25 °C. In these steps, the idea was to determine where the oxygen carrier is able to consume oxygen for its regeneration (oxidation) with an oxygen concentration at least equivalent to that in the surrounding gas. The above temperature-swing procedure was repeated with O_2 concentration of 5 vol%.

Data evaluation

The conversion of the oxygen carrier was calculated as follows:

$$\text{For reduction: } X_{Red} = \frac{m_{Ox} - m}{m_{Ox} - m_{Red}} \quad (2)$$

$$\text{For oxidation : } X_{Ox} = 1 - \frac{m_{Ox} - m}{m_{Ox} - m_{Red}} \quad (3)$$

where m is the sample mass at each time; m_{Ox} is the fully oxidized sample mass and m_{Red} the sample weight in the reduced state.

The initial reaction rate of oxygen release during CLOU was calculated as:

$$r_{O_2}\left(\frac{kgO_2}{kg_{OC}\bullet s}\right) = R_{0,CLOU}\frac{dX_{red}}{dt} \quad (4)$$

and the initial reaction rate of conversion of the oxygen carrier with H_2 and CH_4 were calculated as follows:

$$r_{H_2}\left(\frac{kgO_2}{kg_{OC}\bullet s}\right) = R_{0,CLC}\frac{dX_{red},H_2}{dt} \quad (5)$$

$$r_{CH_4}\left(\frac{kgO_2}{kg_{OC}\bullet s}\right) = R_{0,CLC}\frac{dX_{red},CH_4}{dt} \quad (6)$$

In the thermal cycling experiments for each temperature step, the mass variation was calculated, as well as the conversion considering the CLOU oxygen transport capacity previously measured in isothermal experiments. For all oxygen carriers, the first decrease of the temperature from 950 °C to 800 °C did not shown any change in the weight, because the oxygen carrier samples were completely oxidized. So all the results show data obtained during increasing and decreasing of temperatures of fully oxidized particles with 10 and 5 vol% oxygen during a total of 36 redox cycles.

2.3.2. Batch fluidized bed reactor

The oxygen carrier behavior of the selected oxygen carriers was investigated in a fluidized batch reactor with multiple redox cycles of oxygen release in N_2 and oxidation with different O_2 concentration from 5 to 21 vol% at temperatures from 800 to 950 °C. In this way, the selected particles were exposed to more relevant conditions compared to that in a TGA. Hence, the attrition during redox cycles and the agglomeration trends were determined. A batch fluidized bed reactor setup [36] with a 54 mm inner diameter reactor was used. A batch of 300 g of oxygen carrier particles was used as bed material. The gas feeding system had independent mass flow controllers for different gases.

Tests were carried out with an inlet superficial gas velocity of 0.10 m/s (at 900 °C). Gas composition during reduction was 100 vol% N_2. During oxidation different oxygen concentrations were used ranging from 5 to 21 vol% O_2 in N_2.

The gas outlet downstream from the fluidized bed reactor was connected to two parallel hot filters, with one of them always connected and open towards the gas analyzer system. A para-magnetic gas analyzer (Siemens Oxymat 5E) measured the O_2 concentration evolution with time.

Data evaluation

From the gaseous oxygen concentration, the exit flow, the oxygen carrier conversion as a function of time was calculated:

$$\text{Oxygen Uncoupling } X_{Red}(t) = \int_0^t \frac{F_{O_2}}{N_{O_2}}dt \quad (9)$$

$$\text{Oxidation } X_{Ox}(t) = \int_0^t \frac{1}{N_{O_2}}\left(0.21F_{air} - F_{O_2}\right)dt \quad (10)$$

where X is the oxygen carrier conversion; F_i is the gas i molar flow rate leaving the reactor; N_{O_2} are the molecular oxygen moles which can be released from fully oxidized oxygen carrier by CLOU, and t is the time.

2.4. Attrition evaluation

The attrition resistance of the oxygen carrier was evaluated by two methods: (1) Air Jet Attrition index (AJI) determined in an ATTRI-AS equipment using ASTM-D-5757 standard; and (2) attrition rate measured in the batch fluidized bed reactor. Attrition rate calculation was made from recovered elutriated solids from the bed in a heated filter during the successive reduction–oxidation cycles. The attrition rate was calculated as:

$$A = \frac{m_f}{m_t\Delta t}\bullet 100 \quad (7)$$

where A is the attrition rate (%/h); m_f is the mass of elutriated particles with a particle size lower than 45 μm during a particular period of time, Δt (expressed in hours), and m_t is the total mass of solids in the batch fluidized bed reactor. More information on this setup can be found in [36].

With the attrition rate value obtained it is possible to calculate the extrapolated lifetime of the oxygen carrier by the following equation

$$LT(h) = \frac{100}{A} \quad (8)$$

3. Results

3.1. CLC reactivity of oxygen carrier

Initially the reactivity for CLC of the developed materials was investigated with H_2 and CH_4. The reduction reactivity obtained in the TGA at 800 °C using as reduction agent H_2 and CH_4 was studied for the six oxygen carriers prepared and calcined at 1200 °C due to their good mechanical properties, as can be seen in Table 2. With lower calcination temperatures, only one oxygen carrier showed a crushing strength value higher than 1 N. Fig. 2a shows reduction conversion of the oxygen carrier as a function of the time for the reduction with H_2. From these experiments oxygen transport capacity for CLC reaction was obtained, changing from 5.3 to 9.5 for the different oxygen carriers, see Table 2. For oxygen carriers with only Mg and Mn in their composition, the oxygen transport capacity increased with increasing the Mn content. However, when there is Si in the composition, the increase of Mn content is associated with an increase of Si in the oxygen carrier, and the oxygen transport capacity decreased.

Although the XRD profile indicated that fresh samples contained amorphous phases, and the compounds Mg_6MnO_8, Mg_2MnO_4 and MgO were identified. According with the phases observed and with the literature [30] the following overall reactions are proposed to take place for the reaction with H_2:

$$Mg_6MnO_8 + H_2 \rightarrow 2Mg_{0.5}Mn_{0.5}O + 5MgO + H_2O \quad R_{0,CLC} = 4.9\% \quad (r1)$$

$$Mg_2MnO_4 + H_2 \rightarrow 2Mg_{0.5}Mn_{0.5}O + MgO + H_2O \quad R_{0,CLC} = 9.6\% \quad (r2)$$

According with this, the oxygen transport capacity for CLC reaction would be between 4.9 and 9.6 % depending on the fraction of reactant species present. For the three oxygen carriers with only Mg and Mn the oxygen transport capacity was between both theoretical values, see Table 2.

All the oxygen carriers showed similar reduction reactivity with H_2, with a full conversion in less than 0.5 min. The faster reduction was obtained for the oxygen carrier M24Mg76, followed by M48Mg51, M53Mg44 and M61MgS12.

CLC initial reaction rates obtained with H_2, measured as kg of Oxygen per s and kg of oxygen carrier (kgO/s•kgOC), are presented in Table 2. The higher initial reaction rate with H_2 was found with M48Mg51and M56MgS7, although differences between materials were not important.

In addition, the reduction of oxygen carriers with CH_4 was investigated. Different behavior was found for particles with Si or without Si in the composition. Fig. 2b shows that the oxygen carriers without Si in their composition had higher reactivity than those containing Si, reaching the full conversion in around 4 min. The oxygen carriers with Si in their composition showed low reactivity and needed at least 20 min to reach the full conversion. All the oxygen carriers reached the full conversion, except the M24Mg76, that only reached a reduction conversion

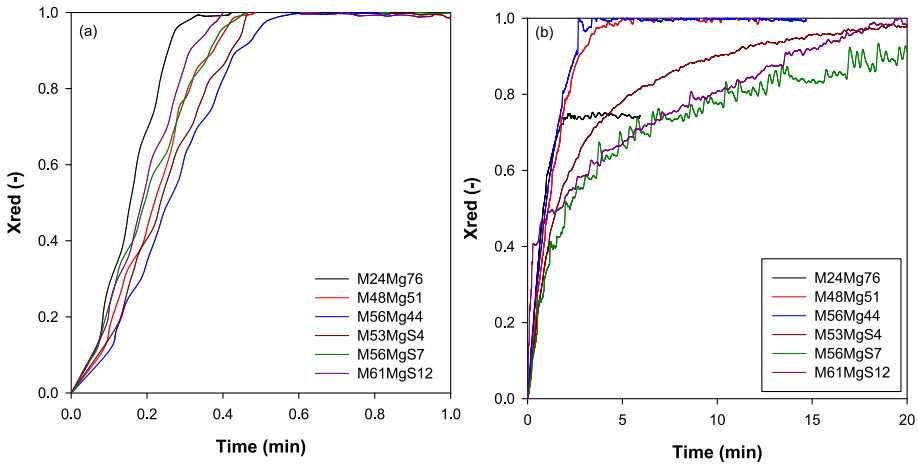

Fig. 2. Oxygen carrier reduction conversion curves with: (a) 15 vol% of H_2; and (b) 15 vol% of CH_4; at 800 °C (N_2 for balance).

of 78 % after 5 min at 800 °C.

Table 2 also shows the initial reaction rates obtained with CH_4. The higher initial rates with CH_4 is obtained with M48Mg51 and M56Mg44. All the oxygen carriers showed a reaction rate with near an order of magnitude lower with CH_4 than with H_2. As a conclusion, it can be seen that for the CLC process using lattice oxygen, the best oxygen carriers are those without Si in their composition and with high Mn in its composition, especially for CH_4 combustion. Hwang et al. analyzed also the reaction rate obtained at 900 °C with CH_4 for two oxygen carriers were the active phase were $MgMnO_3$ and $CaMn_{0.9}Mg_{0.1}O_3$ respectively [30]. Comparing with the materials studied in the present work, the M48Mg51 and M56Mg44 have higher reaction rate than both oxygen carriers. Also, all the oxygen carriers present higher reaction rates than the $CaMn_{0.9}Mg_{0.1}O_3$, except the M61MgS12 [30]. On the other hand, Adánez-Rubio et al. found that the reaction rate at 800 °C with CH_4 was one order of magnitude higher with a Cu-Mn mixed oxide oxygen carrier with kaolin in it composition [37].

3.2. CLOU redox cycling by TGA

In order to analyze the capability of the different oxygen carriers to release oxygen in presence of different concentrations of oxygen in the reaction atmosphere and also the temperature needed to regenerate them with different oxygen concentrations, TGA thermal cycling was made. As the thermodynamics of these materials are not established, this procedure can give a good indication of the optimal temperatures for uptake and release of oxygen, which is important for an optimized CLOU process.

Fig. 3 shows the reduction (Fig. 3a) and oxidation conversions (Fig. 3b) found for the oxygen carrier M24Mg76 at different temperatures in the temperature cycling experiment with a 10 vol% of O_2. During the increase of temperature (reduction), Fig. 3a shows the reduction conversion at temperatures where a discernible variation of weight was found, in this case over 925 °C. Between 925 and 975 °C, the conversion obtained was very small, lower than 4 % for each temperature step. The higher oxygen release was obtained at 1000 °C, so the oxygen concentration at pseudo-equilibrium for this oxygen carrier is higher than 10 vol% between 975 and 1000 °C. After 30 min of reduction at 1000 °C, the oxygen carrier still had oxygen available for release. In addition, the reaction continues at 1025 °C, where after 5 min, the weight was constant. Considering all the weight losses, the total conversion of the CLOU oxygen carrier at this condition was 64 %.

Oxidation of M24Mg76 only begins at 950 °C with 10 vol% of O_2. In the same way as in the reduction, after 30 min, the oxidation was not complete and it continued in the following temperature step (925 °C). In the interval 875–900 °C the oxidation was very slow, with conversions

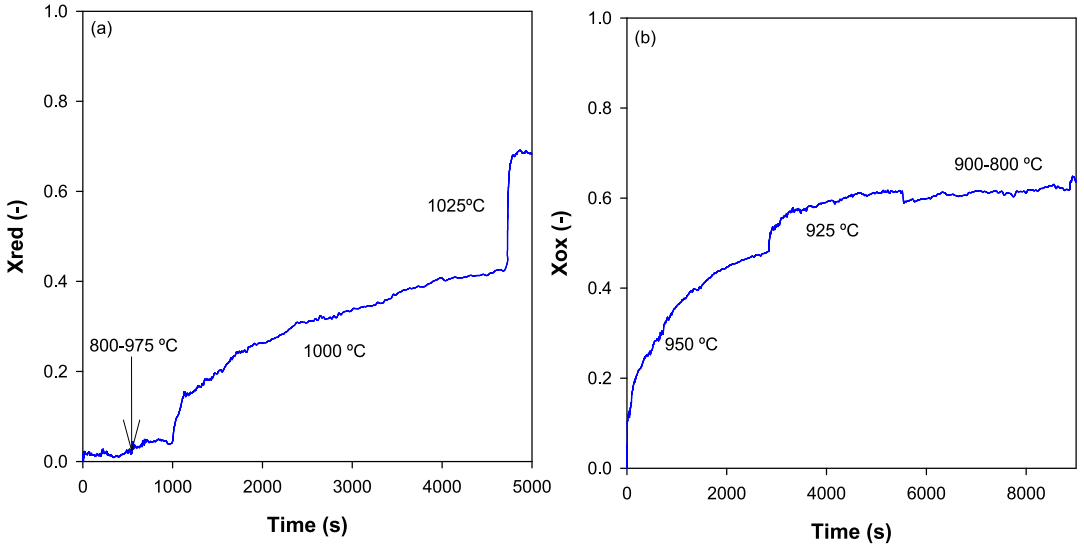

Fig. 3. A) Reduction, i.e. temperature increase, and b) oxidation, i.e. temperature decrease, conversions curves for M24Mg76_1200 oxygen carrier at different temperatures. Samples were exposed to 10 vol% O_2 and 90 vol% N_2.

lower than 5 %, being the oxidation negligible at temperatures lower than 850 °C. The overall weight increase during oxidation was 64 % indicating that the total oxygen recovered during the oxidation was the same as that released during the reduction.

Fig. 4 shows the results found with 5 vol% of O_2 in the gas. The reduction (Fig. 4a) and oxidation conversion (Fig. 4b) are shown as a function of time for the oxygen carrier M24Mg76 in the temperature cycling experiment. The same behavior as that found with 10 vol% of O_2 was observed in the temperature interval of 800 to 975 °C, i.e. the conversion obtained was lower than 5 % for each temperature step. The higher oxygen release was obtained at 975 and 1000 °C. So the oxygen concentration at pseudo-equilibrium for this oxygen carrier had values higher than 5 vol% at atmospheric pressure between 950 and 975 °C. As after 30 min of constant temperature, the oxygen carrier still had oxygen available for release. Moreover, the reaction continues at 1000 °C, where after 10 min the weight was stabilized. The total conversion of the oxygen carrier at this condition was 64 %, similar to that obtained in the cycles carried out with a 10 vol% of O_2. Thus, it is expected that this fraction of the oxygen transport capacity is released at high rates at usual CLOU conditions.

The oxidation begins at 925 °C, similar to where the reduction was initiated. As the oxidation was not complete it continued in the following temperature step (900 °C). In the interval 900–800 °C the oxidation was very small, with conversions lower than 5 %. In this case the oxygen was not completely recovered during the oxidation. In this case the oxidation at 900 °C was so slow that it was cut after 15 min, and it is possible that the oxygen carrier needs additional time to complete the oxidation.

In the case of the oxygen carriers with higher fractions of Mn, i.e., M48Mg51 and M56Mg44, with a 10 vol% O_2 in the interval 800–1000 °C the weight variation was negligible. At 1025 °C the maximum oxygen release was measured, with an oxygen carrier conversion of 35 % and 25 % respectively. Therefore, the oxygen concentration at pseudo-equilibrium for both oxygen carriers is higher than 10 vol% between 1000 and 1025 °C. With a 5 vol% of O_2, for both oxygen carriers in the interval 800–975 °C the weight variation was significantly lower, around 4 %. At 1000 °C, the maximum oxygen release, with an oxygen carrier conversion of 35 % and 25 % was found with M48Mg51 and M56Mg44 respectively, more or less equal to that obtained in the cycles carried out with 10 vol% of O_2 in the gas mixture. So the oxygen concentration at pseudo-equilibrium for these oxygen carriers is higher than 5 vol% between 975 and 1000 °C.

The oxidation occurred at 950 °C (10 vol% O_2) and 925 °C (5 vol% O_2), and it was complete after 27 and 25 min, respectively. In the interval 900–800 °C the oxidation was very small, with conversions lower than 5 %. Also, it can be seen than the total oxygen recovered during the oxidation was slightly lower than that released during the reduction. The oxidation conversion was 32 and 23 % respectively, following of a reduction conversion of 35 and 25 % obtained with oxygen concentrations of 5 and 10 % respectively. Hence, it can be considered that at this condition near all the oxygen released was recovered.

In the case of the oxygen carriers with Si in their composition, the reduction and oxidation conversion in the cycling experiments carried out in the TGA were very poor. Only M53MgS4 showed a total conversion of 12 % at 1025 °C (10 vol% O_2) and at 1000 °C (5 vol% O_2). The oxidation was occurred at 950 °C (10 vol% O_2) and 925 °C (5 vol% O_2). However, only a 60 % of the total oxygen was recovered from the oxygen released in the previous reduction in both cases. In the case of the M56MgS7 and M61MgS12 in the interval 800–1025 °C, no reactivity with both oxygen concentrations was observed. M56MgS7, showed good reactivity in the TGA analysis carried out without oxygen at 950 °C with N_2, therefore it is likely necessary with a higher temperature than 1025 °C to observe the oxygen concentration at pseudo-equilibrium. Hence, for this oxygen carrier, the equilibrium concentrations at a given temperature are likely higher than 5 and 10 vol% O_2 at investigated temperatures.

In summary, the temperature swing experiments give a picture of the oxygen release and absorption pattern for this new type of oxygen carriers. It is clear that the reduction temperature when there is oxygen in the reduction atmosphere depend on the oxygen concentration, in general the reduction starts at 1000–1025 °C with 10 vol% and at 975–1000 °C with a 5 vol% of O_2. At these conditions, the oxygen concentration at pseudo-equilibrium is higher than the oxygen concentration present in the reaction atmosphere. Similar situation happens for the oxidation, where the oxidation begins when the oxygen carrier reaches 950 °C (10 vol% O_2) and 925 °C (5 vol% O_2). It appears as if higher Mn content increases the equilibrium temperature for phase transition, see Fig. 4. Similarly, the addition of Si to the lattice also affects the release pattern of oxygen, and seems to increase the equilibrium concentration for the phase transition.

3.3. CLOU reactivity at isothermal conditions

CLOU reduction and oxidation reactivity was obtained in the TGA between 850 and 950 °C for the six oxygen carriers selected. The reduction and oxidation were measured at the same temperature and with a gas composition of 100 vol% N_2 for the reduction and air for the oxidation. All the oxygen carriers showed the same behavior, an increase of the reduction reactivity with higher temperature.

The experimental oxygen transport capacity for CLOU reaction for all the oxygen carriers, except for M61MgS12, were similar, between 2 and 2.5 %, increasing when the Mn content in the particles increased, see

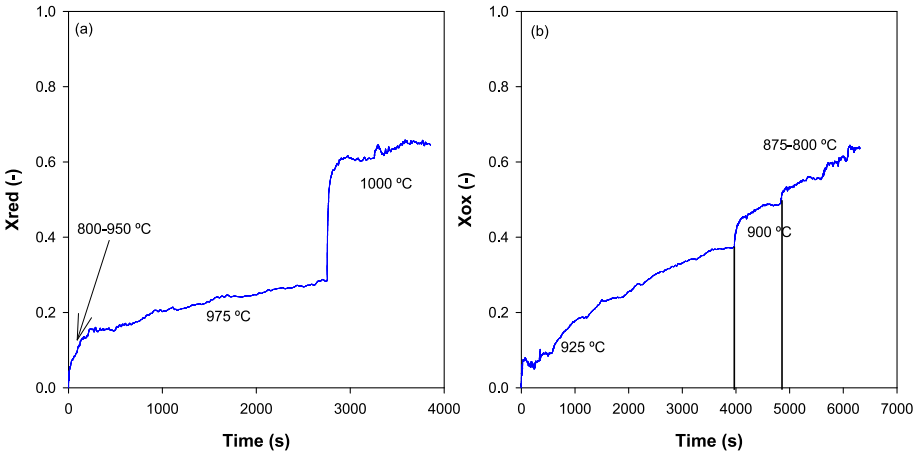

Fig. 4. A) Reduction, and b) oxidation conversions for M24Mg76_1200 oxygen carrier at different temperatures. Gaseous environment consisted of 5 vol% O_2 and 95 vol% N_2.

Table 2. According with the phases detected by XRD, the CLOU reaction that take place could be the following:

$$4Mg_6MnO_8 \rightarrow 2MgMn_2O_4 + 22MgO + O_2 \quad R_{0,CLOU} = 2.4\% \quad (r3)$$

$$4Mg_2MnO_4 \rightarrow 2MgMn_2O_4 + 6MgO + O_2 \quad R_{0,CLOU} = 4.8\% \quad (r4)$$

The oxygen transport capacity for CLOU reaction varied between 2.4 and 4.8 % depending on the reactant species. According with the literature, several days of continue reduction without fuel (H_2 or CH_4) reaction are necessary to obtain $Mg_{0.5}Mn_{0.5}O$ [28], but it was not observed in the experiments carried out here. Table 2 shows that for M24Mg76 and M48Mg51 the oxygen transport capacity for CLOU were slightly lower than those obtained for Mg_6MnO_8 decomposition, likely due to the highly amorphous compounds. Not all the oxygen available for CLOU was released and the oxygen carriers could have some activation by redox cycles. In the case of M56Mg44, the experimental CLOU oxygen transport capacity was slightly higher than for Mg_6MnO_8. Moreover, the highly amorphous content in the sample makes possible that other mixed oxides could be present and not detected by the XRD analysis.

Fig. 5 shows the reduction (Fig. 5a) and oxidation (Fig. 5b) conversion curves for the five oxygen carriers studied. M61MgS12 showed only CLOU properties in the first reduction cycle, in the following oxidation the oxygen carrier was not able to recover the oxygen released during the reduction, therefore it was not plotted in Fig. 5 and therefore, the M61MgS12 is not considered as suitable for the CLOU process.

M24Mg76 and M48Mg51 were the more reactive oxygen carriers, which reached the maximum conversion in less than 10 min. The other three oxygen carriers, all with higher Mn content, need the double of time to reach the maximum conversion. However, maximum values of CLOU oxygen transport capacity, see Table 2, were obtained with materials with higher Mn content as M56MgS7, followed by M56Mg44 and M48Mg51. Although the CLOU oxygen transport capacity obtained for M24Mg76 was one of the lowest (2.0 %) due to the low amount of Mn in their composition, its mass-based conversion rate was similar to the oxygen carriers with more than double the Mn content in their composition, see Table 1.

Results found for the oxygen carrier oxidation carried out in the TGA with air (21 vol% of O_2) at the same temperature than the reduction (950 °C), are plotted in Fig. 5b. For the five oxygen carriers, the oxidation was complete up to the value reached in the previous reduction during the same cycle. Therefore, these oxygen carriers are able to recover in air all the oxygen released during the reduction reaction, even at 950 °C. Moreover, in all cases the oxidation was much faster than the previous reduction. This behavior was obtained in all the temperature intervals studied. Thus, it can be said that oxygen carriers: M24Mg76, M48Mg51 and M56Mg44 looks suitable for further investigation due to its high reactivity and acceptable crushing strength, see Table 2. M53MgS4 and M56MgS7 showed a good reactivity but their low crushing strength make these materials unsuitable for the process, at least not with respect to the current production procedure, see Table 2.

Table 3 summarizes the main results obtained in the thermal cycling for the oxygen carriers with Mn-Mg mixed oxides, which were reactive both in N_2 and with 5/10 vol% of O_2. The samples with Si showed a very poor behavior in the thermal swing experiments and are thus not included in Table 3. The three samples with high $R_{OC,eff}$ and with crushing strength values higher than 1 N were investigated with more detail, and thus they should be suitable to be investigated in the batch fluidized bed reactor with respect to the oxygen release rate and the regeneration of the oxygen carrier particles. Table 3 shows that it is highly dependent on the TGA operating conditions. All the samples showed a similar oxygen release rate in N_2 atmosphere, with values of $0.1 \bullet 10^{-3}$ kg O_2/s•kg OC, at 950 °C. In the thermal swing experiments, the oxygen carrier M24Mg76 released oxygen at lower temperatures than M48Mg51and M56Mg44, but this release was one order of magnitude slower. However, if the release was measured at the same temperature used for M48Mg51 and M56Mg44 (1000–1025 °C). The M24Mg76 oxygen release rate was 2 times higher.

With the maximum conversion value obtained in the TGA in the cycles carried out with 5 and 10 vol% of O_2, the effective oxygen transport capacity can be calculated, $R_{OC,eff}$.

Table 3 shows that the oxygen carrier that has the better value was M24Mg76 with an oxygen conversion or exploitation of 65 % which has an effective oxygen transport capacity ($R_{OC,eff}$) of 1.3 %, followed by the M48Mg51 with a 0.9 % with and oxygen exploitation of 35 %,while the M56Mg44 only obtained 25 % conversion in the investigated temperature range. Thus, the more suitable materials for scale up to the batch fluidized bed were:

- M24Mg76 due to its high reactivity, good oxygen transport capacity and the best effective oxygen transport capacity. This oxygen carrier is able to release oxygen at lower temperatures than the rest of the oxygen carriers analyzed.
- M48Mg51 was also judged as viable, due to its high reactivity, good oxygen transport capacity and its acceptable crushing strength.

3.4. Batch fluidized bed reactor tests

Two oxygen carriers (M24Mg76 and M48Mg51) were selected for batch fluidized bed reactor testing. New batches of both oxygen carriers were prepared and calcined. However, to obtain good values of crushing strength it was necessary to calcine at 1225 °C during 6 h, see Table 4. After 6 h of calcination instead of 2, both oxygen carriers showed almost

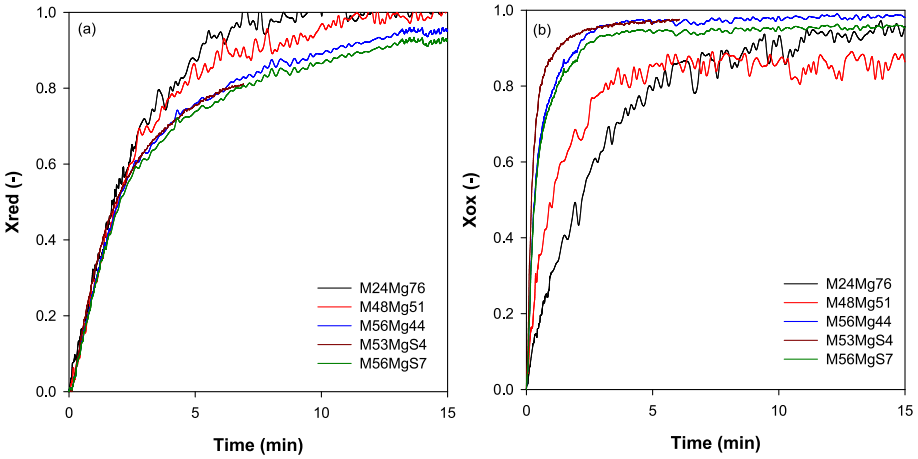

Fig. 5. CLOU behavior of oxygen carriers (a) reduction and (b) oxidation conversion curves at 950 °C. Reduction: N_2; Oxidation: 21 vol% O_2 in N_2.

Table 3
Main results obtained with the oxygen carriers studied with Mn-Mg mixed oxides using the TGA.

Oxygen carrier	Crushing strength (N)	R_{OC} (%)	$R_{OC,eff}$ (%)	TGA conditions	Temperature	$r_{O_2} \bullet 10^3 (kgO_2/s \bullet kgOC)$
M24Mg76	1.16	2.0	1.3 (65 %)	100 vol% N_2	950 °C	0.10
				5 vol% O_2	975/1000 °C	0.008/0.05*
				10 vol% O_2	1000/1025 °C	0.007/0.05*
M48Mg51	1.94	2.3	0.9 (35 %)	100 vol% N_2	950 °C	0.10
				5 vol% O_2	1000 °C	0.03*
				10 vol% O_2	1025 °C	0.03*
M56Mg44	1.16	2.45	0.6 (25 %)	100 vol% N_2	950 °C	0.11
				5 vol% O_2	1000 °C	0.02*
				10 vol% O_2	1025 °C	0.02*

* Results obtained in the temperature cycling experiments.

Table 4
Main properties of the M24Mg76 and M48Mg51 oxygen carriers fresh and used (25 h) in the batch fluidized bed reactor.

Oxygen carrier	$R_{0,CLOU}$ (%)		Crushing strength (N)		AJI (%)	
	Fresh	Used	Fresh	Used	Fresh	Used
M24Mg76	1.9	2.4	1.5	1.4	0.2	0.9
M48Mg51	2.3	2.3	1.4	1.3	0.3	0.8

the same value of oxygen transport capacity with both calcination conditions. For the batch fluidized bed reactor test, 300 g of spray dried oxygen carrier were used in the size range +0.1–0.3 mm. The oxygen release behavior of both oxygen carriers was analyzed. Moreover, the resistance to the agglomeration and attrition at high temperature during 25 h of hot fluidization was analyzed with each oxygen carrier.

Fig. 6 shows, as one example, the oxygen concentration profiles measured during multiple redox cycles carried out with the oxygen carrier M24Mg76 at 850, 900 and 950 °C. When N_2 was fed to the reactor, the oxygen concentration falls from 21 to values near to 1 (850 °C), 1.3 (900 °C) and 2.5 vol% (900 °C) respectively. These values decreased with time. This decrease was more accentuated at temperatures lower than 950 °C, and at this temperature the oxygen concentration was more stable with respect to time, with values close to 2 vol%. This behavior was observed in the three cycles carried out at each temperature. In addition, it can be appreciated that the oxidation with air was fast in all the interval of the temperatures studied. Similar results were obtained with the oxygen carrier M48Mg51. Some differences in the concentration of oxygen released were observed, but in general terms both oxygen carriers showed a similar behavior. None of the oxygen carriers showed any agglomeration problem during the 25 h of hot fluidization carried out.

The concentration of oxygen released and the reactivity during several redox cycles for both oxygen carriers were investigated. Fig. 7 shows the oxygen concentration at the reactor outlet stream (Fig. 7a) together with the oxygen carrier reduction conversion (Fig. 7b) found at different temperatures for the oxygen carrier M24Mg76. When the temperature increases the concentration of oxygen released also increased, with subsequent increase of the oxygen carrier reduction. The oxygen concentration released by the oxygen carrier decreased with time at temperatures lower than 950 °C, following a behavior observed for mixed oxide oxygen carriers [8,17,18,29,31,38]. At 950 °C, the oxygen concentration was highly stable with the time, similar to that found with single oxide oxygen carriers with clear phase transitions

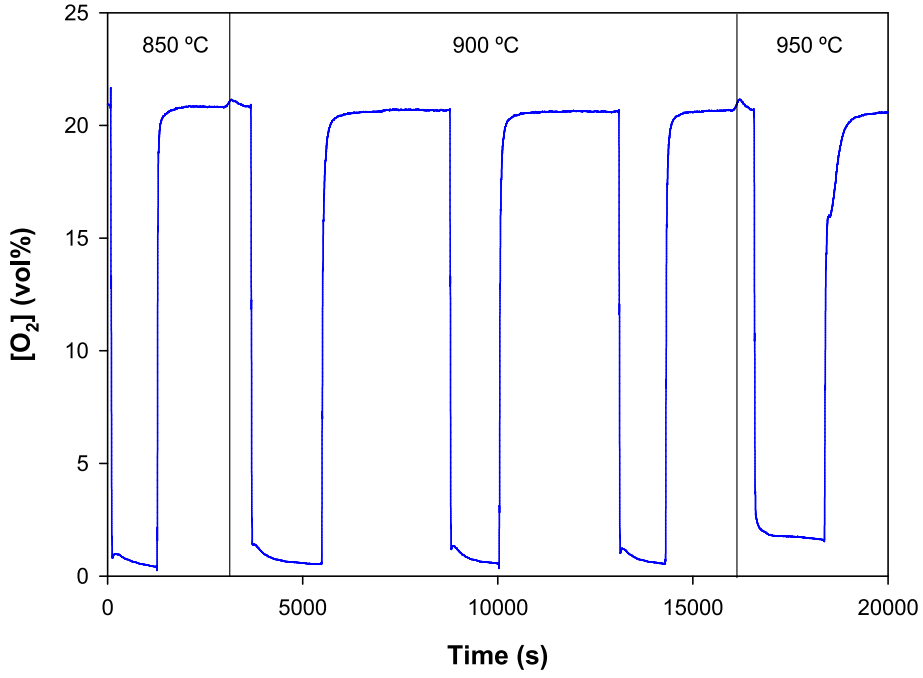

Fig. 6. Oxygen concentration measured during multiple redox cycles carried out in the batch fluidized bed at 850, 900 and 950 °C. Oxygen carrier M24Mg76. Reduction: N_2; Oxidation: 21 vol% O_2 in N_2.

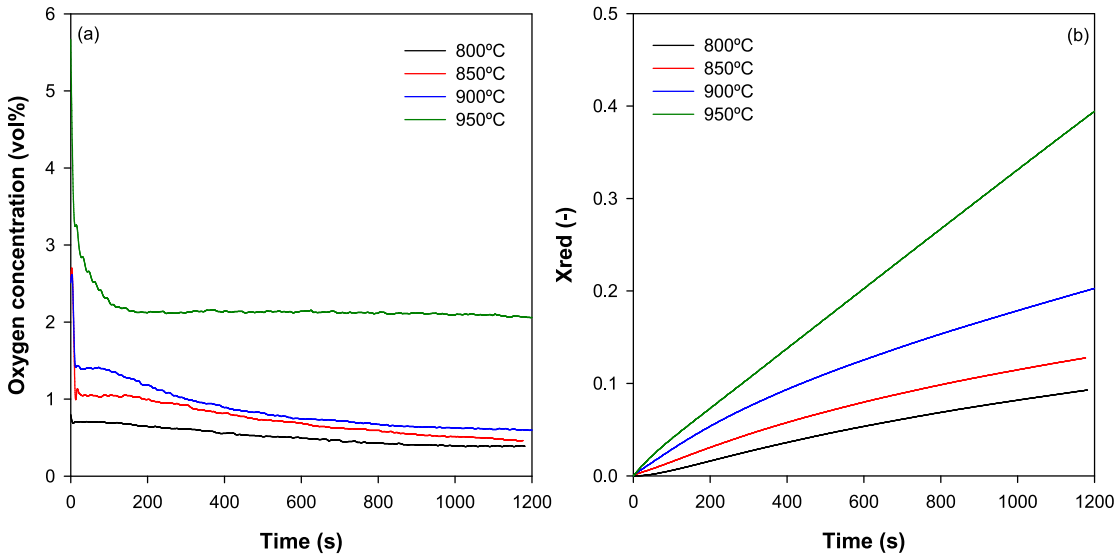

Fig. 7. Oxygen uncoupling cycles at different temperatures carried out with M24Mg76 in the batch fluidized bed reactor: a) oxygen concentration; and b) solid conversion. Air for oxidation.

[36,39,40]. The solid conversion found was low operating at temperatures lower than 950 °C. Note that after 20 min of reaction, 35 % of the oxygen carrier conversion was obtained at this temperature.

Similar behavior was obtained with the oxygen carrier M48Mg51, Fig. 8. The increase of the temperature, increased the oxygen concentration in the batch fluidized bed reactor outlet (Fig. 8a), increasing the oxygen carrier conversion (Fig. 8b). The main difference observed was that the total amount of oxygen at pseudo-equilibrium released by M48Mg51 was higher than the one found with M24Mg76. This was due to the higher Mn content of the former material, having a higher oxygen capacity at this temperature. At 950 °C, while the M24Mg76 reached quickly the pseudo-equilibrium oxygen concentration, M48Mg51 needs 600 s to reach the pseudo-equilibrium oxygen concentration, as a perovskite material [31] or a Cu-Mn mixed oxide [38], and this value was slightly lower than that obtained with M24Mg76.

With respect to the oxygen carrier conversion during the reduction, it can be observed that the higher oxygen release obtained with the M48Mg51 involved a higher oxygen carrier reduction conversion at 800 (13 % instead of 9 %) and at 850 °C (16 % compared to 12 %). However, at 900 °C the oxygen carrier conversion was similar for both oxygen carriers, and at 950 °C the conversion of the M24Mg76 was higher than the M48Mg51. Moreover, at 950 °C after 20 min of reduction the oxygen released by the M24Mg76 was slightly higher than with M48Mg51, 2.5 g compared to 2.3 g of oxygen respectively per 100 g of oxygen carrier. This behavior could be related with the effective oxygen transport capacity found in the TGA with N_2 at 950 °C that was higher for the M24Mg76 (1.3 %) than for M48Mg51 (0.9 %).

The effect of the oxygen concentration during the oxygen carrier oxidation at 850 °C for both oxygen carriers was also analyzed, see Fig. 9. Dotted lines represent the reduction conversion reached in the previous cycle. M24Mg76 was fully regenerated with 21 and 10 vol% of O_2, recovering all the oxygen released in the previous reduction (Fig. 9a). However, with a 5 vol% of O_2, in the first oxidation cycle the oxygen carrier was not able to recover all the O_2 released in the previous reduction, losing 26 % of oxygen. In the following cycle carried out in the same conditions, the oxygen carrier released lower amount of

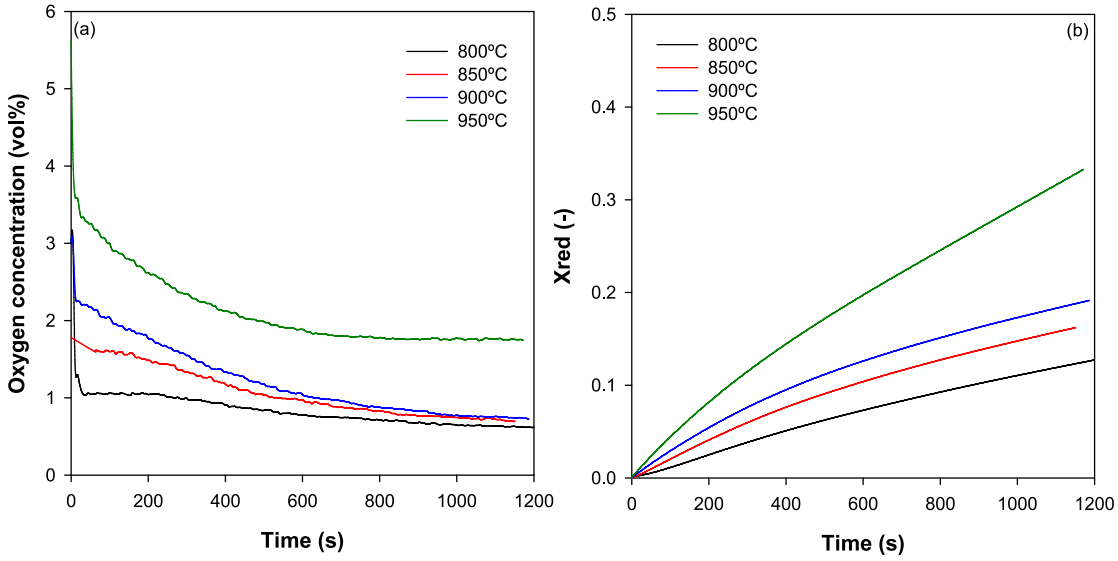

Fig. 8. Oxygen uncoupling cycles at different temperatures carried out with M48Mg51 in the batch fluidized bed reactor: a) oxygen concentration; and b) solid conversion. Air for oxidation.

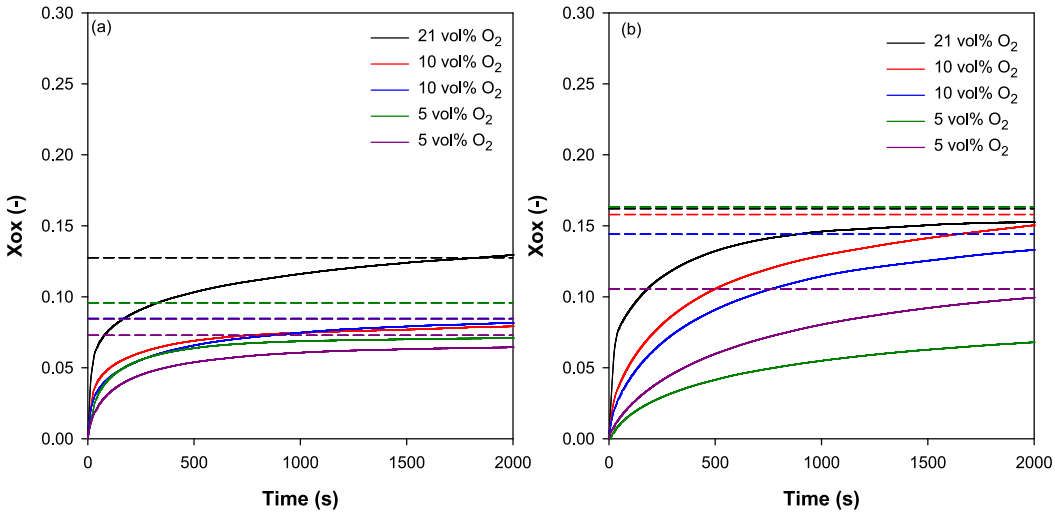

Fig. 9. Effect of the oxygen concentration on the oxygen carrier conversion during the oxidation at 850 °C in the batch fluidized bed reactor: (a) M24Mg76, (b) M48Mg51. Oxidation conversion (—); Reduction conversion in the previous reduction (- - -).

oxygen, with a lower reduction conversion. In the oxidation of the second cycle, again, the oxygen carrier was not able to be fully regenerated, but losing less amount of O_2 (11 %).This behavior can be likely due to kinetic limitations originated when the conversion increases.

On the other hand, the oxygen carrier M48Mg51 showed a similar behavior in the oxidation with air. However, in the oxidation with 10 and 5 vol% the oxygen carrier was not able to recover all the oxygen released in the previous reduction, losing between 5 and 50 % of the oxygen released in the previous reduction (Fig. 9b). The highest loss was found in the first oxidation, reaching a 50 % in the first cycle when regeneration was carried out with 5 vol% of O_2. In the second oxidation, the oxygen carrier lost lower amount of oxygen with both oxygen concentrations, around 5 %. Therefore, both oxygen carriers were able to release enough oxygen at different temperatures. However, M24Mg76 can be fully regenerated with O_2 concentrations higher than 5 vol%, while for M48Mg51, at the same operating conditions, need 21 vol% of O_2 to be fully regenerated in a reasonable amount of time. This behavior could be related with the behavior found in the TGA during the thermal cycling where it was found that with 10 vol% of O_2, the M24Mg76 was able to recover all the oxygen released during reduction but it was not possible with the M48Mg51. However, in the TGA the M24Mg76 can be fully regenerated with 5 vol% of O_2, and in the batch fluidized bed reactor neither of both can recover all the oxygen previously released.

In the experiments carried out in the batch fluidized bed reactor, the attrition rate of both oxygen carriers was measured, with the fines elutriated from the reactor and recovered by hot filters. Fig. 10 indicates that the initial values of the attrition rate were low for both oxygen carriers. For M24Mg76 the attrition rate suffers a slight decrease in the first 20 h of hot fluidization, however, after 25 h the attrition rate suffers a big increase, being the last value of 0.05 %/h. For M48Mg51 the attrition rate decreased with the operation time, from 0.025 to 0.004 %/h. This value is 10 times lower than that obtained after 25 h with M24Mg76. Extrapolated lifetimes obtained from attrition rates obtained in a batch fluidized bed reactor can be only used for comparison between both materials, because are not obtained in a complete CLC system nor any fuel was used. For the M24Mg76 even with the increase of the attrition rate, the extrapolated lifetime would be estimated to 2000 h, and for M48Mg51 it would be estimated to 25000 h. However, previous experience indicated that these values are highly reduced when oxygen carriers are used in continuous units with interconnected fluidized bed reactors [36].

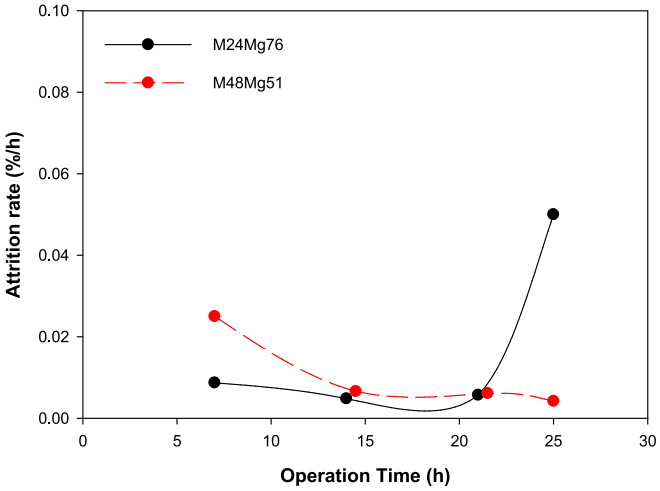

Fig. 10. Attrition rate as a function of the hours of operation of the oxygen carriers studied in the fluidized bed reactor: M24Mg76 and M48Mg51.

3.5. *Oxygen carrier characterization after use*

After the experiments carried out in the batch fluidized bed reactor both oxygen carriers were characterized. The CLOU reactivity was measured in the TGA, as well as the crushing strength and the AJI. Fig. 11 shows the reduction curves obtained in the TGA tests carried out with N_2 at 950 °C. For M24Mg76 the maximum conversion obtained after 25 h in the batch fluidize bed increased. This means that the oxygen carrier was activated during the CLOU cycles in the batch reactor, increasing the oxygen transport capacity by 25 %, from 1.9 to 2.4, slightly higher than that obtained with the M48Mg51 material, see Table 4. In the case of M48Mg51, the reactivity and the oxygen transport capacity were near the same after 25 h of hot fluidization in the batch fluidized bed reactor.

Table 4 shows the crushing strength and the AJI index of the particles used. The crushing strength of both oxygen carriers suffer from an almost negligible decrease of 0.1 N. The attrition Jet Index (AJI) was low for both oxygen carrier materials (see Table 4), and suffered a slight increase, although the final values were far away from the maximum AJI value considered as acceptable for fluid catalytic cracking (FCC) catalysts (AJI $\leq$ 5 %) [34]. Both parameters indicate that the mechanical

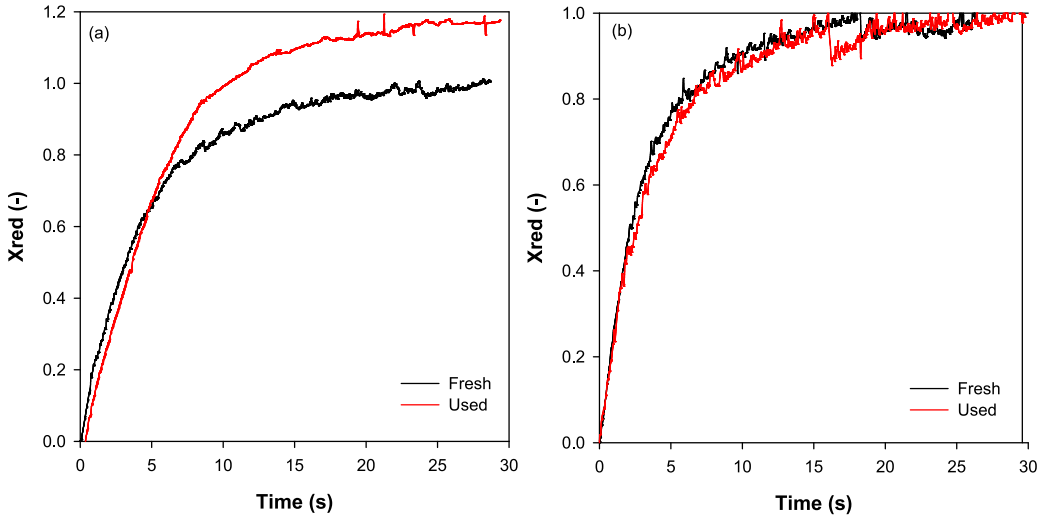

Fig. 11. Results from TGA reduction with N_2 at 950 °C for fresh and used (batch fluidized bed) oxygen carrier: (a) M24Mg76; and (b) M48Mg51.

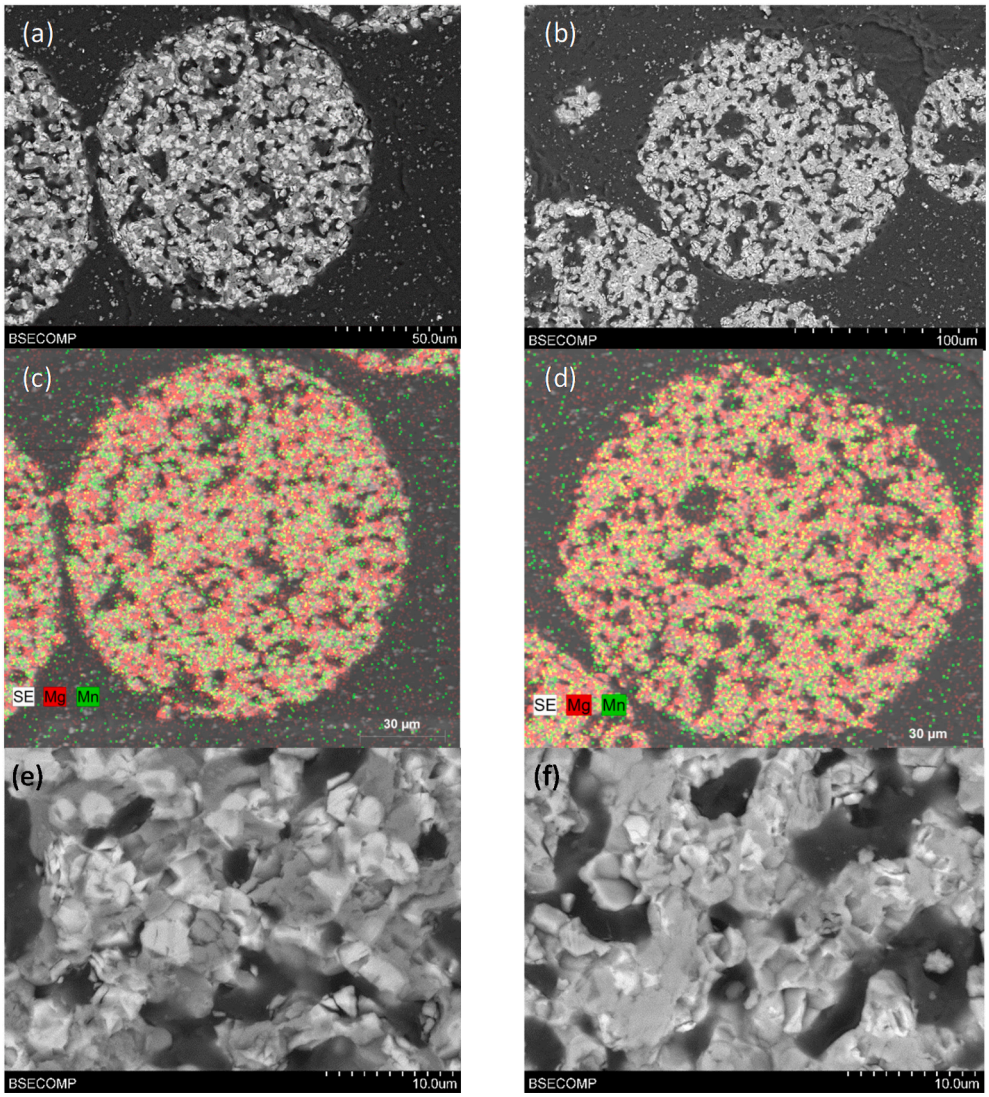

Fig. 12. SEM images of fresh (left) and used particles of M24Mg76 after 25 h in the batch fluidized bed reactor for N_2-air (right): (a, b) cross section of a particle; (c, d) mapping of the inner of the particle; (e, f) surface image of the oxygen carrier particle.

stability of the particles of both oxygen carriers is high and it was maintained during continuous redox cycles.

Thus it can be said that the oxygen carriers M24Mg76 and M48Mg51 had a good behavior with respect to the CLOU reactivity, and mechanical stability in the batch fluidized bed reactor. However, values of at least 10 vol% of O_2 were needed to regenerate both oxygen carriers. Both show no agglomeration problems and the attrition rate was low, obtaining high extrapolated lifetime values. Moreover, M24Mg76 showed activation during the experiments in the batch fluidized bed reactor experiments, increasing the oxygen transport capacity by 25 %.

SEM-EDX analysis was done on fresh and used particles of M24Mg76 (Fig. 12) and M48Mg51 (Fig. 13) oxygen carriers.

The particles of both oxygen carriers had rounded shape with holes in the interior of the fresh particles (Figs. 12a and 13a) and also in the used ones (Figs. 12b and 13b). Moreover, Mg and Mn were well distributed in the inner of the particles of fresh and used particles for the M24Mg76 (Fig. 12c and 12d) and for the M48Mg51 (Figs. 13c and 13d).

In the case of M24Mg76 fresh particles, the surface of the particles shows crystals of two different colors, the bright ones were enriched in Mn and the dark ones were mainly Mg, see Fig. 12e. This difference was also observed in the inner of the particles (not shown). In the used particles of M24Mg76 (Fig. 12f), the different crystals almost

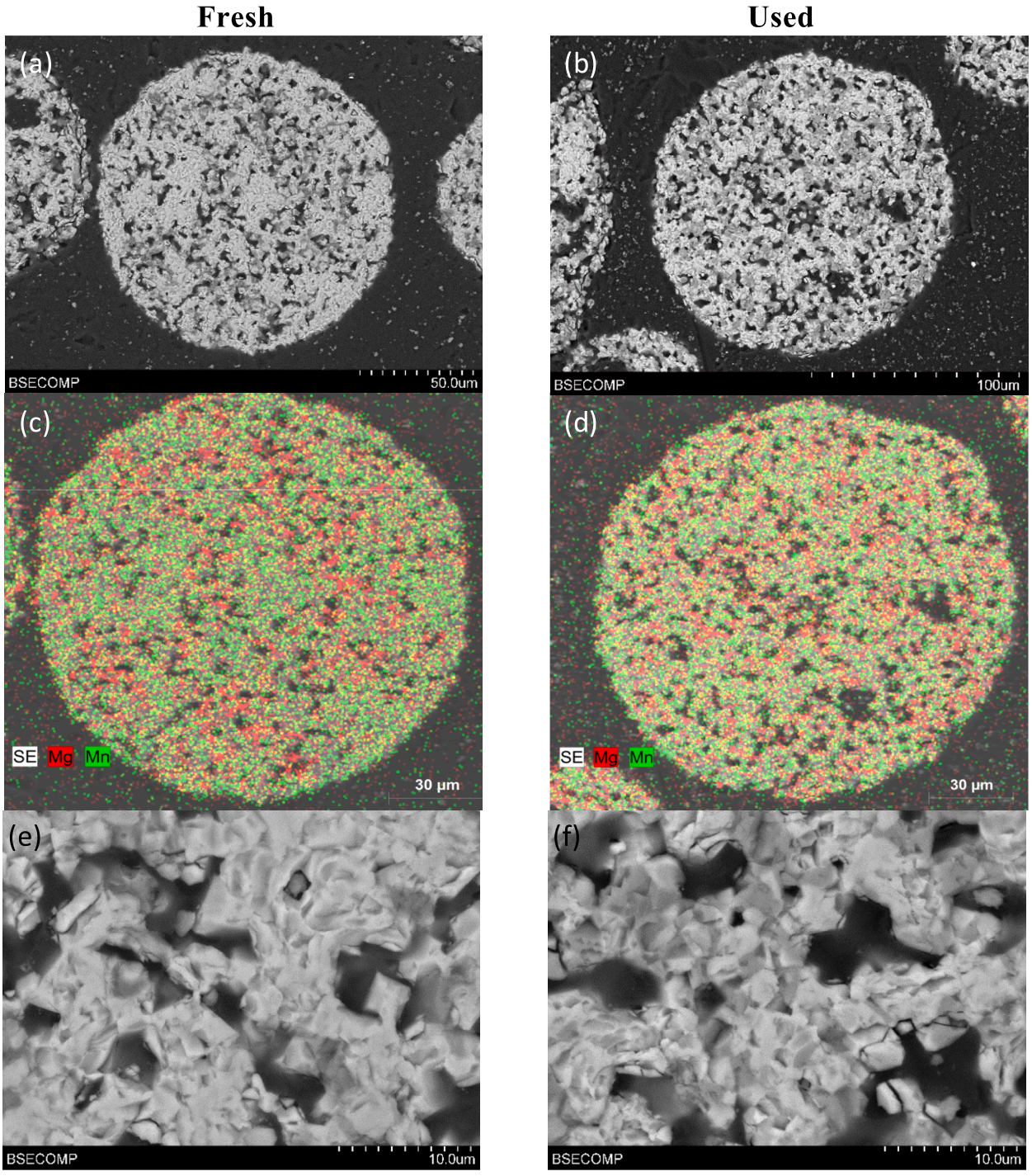

Fig. 13. SEM images of fresh (left) and used particles of M48Mg51 after 25 h in the batch fluidized bed reactor for N_2-air (right): (a, b) cross section of a particle; (c, d) mapping of the inner of the particle; (e, f) surface image of the oxygen carrier particle.

disappeared and all crystals analyzed had very similar composition. Therefore, the crystal form changed during the redox cycles in the batch fluidized bed reactor, and this could be related with the increase of oxygen transport capacity of M24Mg76, see Fig. 11a. With respect to the M48Mg51 oxygen carrier, the crystals found in the inner and the surface of the particles had similar composition in the fresh and used particles, with small differences in the color of the crystals, see Fig. 13e and 13f.

4. Conclusions

In the present work, six different mixed oxides of the system Mn/Mg/Si, that uses very cheap oxides, were investigated for the CLC process. The effect of the Mn fraction, and the effect of the presence of Si in the composition together with the calcination temperature were analyzed in order to know their CLC and CLOU properties.

The oxygen transport capacity for lattice oxygen were significant, up to 9.5 % for Mn56Mg44 and Mn56MgS7 oxygen carriers. CLC reactivity with CH_4 is higher with Mn/Mg oxygen carriers and increases with the Mn content, being the maximum with Mn56Mg44. Complete conversion was obtained with all the oxygen carriers except for M24Mg76.

CLOU oxygen transport capacity was from 2 to 2.5 increasing with the Mn content of the oxygen carrier, a number which should be sufficient for a well-functioning process. Based on XRD analysis, the active phases for CLOU reactions were likely, systems $Mg_6MnO_8/MgMn_2O_4$ and $MgMnO_4/MgMn_2O_4$. The most reactive oxygen carriers for the CLOU process were M24Mg76 and M48Mg51. The oxygen release rate at 950 °C was similar for all the oxygen carriers except for M61MgS12 and can be regenerated with air at this temperature.

Temperature cycling by TGA with increasing/decreasing of temperature at 25 °C steps indicate that, as expected, O_2 release rate decreased with the oxygen concentration in the atmosphere (5/10 vol %). M24Mg76 was able to generate oxygen at lower temperatures. For the oxidation, the temperature to regenerate the oxygen carriers with a 5 vol% of O_2 was 925 °C and 950 with a 10 vol% of O_2. It was also observed that for the oxygen carriers with Si in the composition, the regeneration was very poor.

M24Mg76 and M48Mg51 were selected for scale up to the batch fluidized bed reactor due to their high reactivity, good oxygen transport capacity and good crushing strength. Moreover, both oxygen carriers showed good behavior respect to the CLOU reactivity, and mechanical stability. However, values of at least 10 vol% of O_2 were needed to regenerate both oxygen carriers at 850 °C, something which could be an issue for an efficient power cycle, i.e. high oxygen concentrations are needed in outlet of air reactor. No agglomeration problem was found with both oxygen carriers and the attrition rate was low, obtaining high-extrapolated lifetime values. Moreover, the M24Mg76 showed activation during the experiments in the batch fluidized bed reactor experiments, increasing the oxygen transport capacity by 20 %.

CRediT authorship contribution statement

Iñaki Adánez-Rubio: Conceptualization, Investigation, Methodology, Data curation, Validation, Writing – original draft, Writing – review & editing. **Tobias Mattisson:** Conceptualization, Resources, Validation, Writing – review & editing, Funding acquisition. **Marijke Jacobs:** Writing – review & editing. **Juan Adánez:** Resources, Writing – review & editing, Supervision, Funding acquisition.

Declaration of Competing Interest

The authors declare that they have no known competing financial interests or personal relationships that could have appeared to influence the work reported in this paper.

Data availability

Data will be made available on request.

Acknowledgment

The work presented in this article is partially funded by the Spanish Research Council (CSIC) through the Intramural Project (201980E043). I. Adánez-Rubio acknowledges for “Juan de la Cierva” Program (Grant IJC2019-038987-I funded by MCIN/AEI/10.13039/501100011033). The work was also supported by Chalmers Energy Area of Advance.

References

[1] Project CC. Carbon dioxide capture for storage in deep geologic formations –results from the CO2 capture project. CCS Technology Development and Demonstration Results (2009-2014). CPL Scientific; 2015.
[2] Abad A, Adánez-Rubio I, Gayán P, García-Labiano F, de Diego L, Adánez J. Demonstration of chemical-looping with oxygen uncoupling (CLOU) process in a 1.5 kW_{th} continuously operating unit using a Cu-based oxygen-carrier. Int J Greenhouse Gas Control 2012;6:189–200.
[3] Adánez-Rubio I, Abad A, Gayán P, de Diego LF, García-Labiano F, Adánez J. Performance of CLOU process in the combustion of different types of coal with CO_2 capture. Int J Greenhouse Gas Control 2013;12:430–40.
[4] Adánez-Rubio I, Abad A, Gayán P, de Diego LF, García-Labiano F, Adánez J. Biomass combustion with CO_2 capture by chemical looping with oxygen uncoupling (CLOU). Fuel Process Technol 2014;124:104–14.
[5] Imtiaz Q, Hosseini D, Muller CR. Review of oxygen carriers for chemical looping with oxygen uncoupling (CLOU): thermodynamics, material development, and synthesis. Energ Technol 2013;1(11):633–47.
[6] Adánez-Rubio I, Gayan P, Abad A, de Diego LF, García-Labiano F, Adánez J. Coal combustion by a spray granulated Cu-Mn mixed oxide for CLOU process. Appl Energy 2017;208:561–70.
[7] Adánez-Rubio I, Abad A, Gayan P, de Diego LF, Adánez J. CLOU process performance with a Cu-Mn oxygen carrier in the combustion of different types of coal with CO_2 capture. Fuel 2018;212:605–12.
[8] Adánez-Rubio I, Abad A, Gayán P, Adánez I, de Diego LF, García-Labiano F, et al. Use of hopcalite-derived Cu-Mn mixed oxide as oxygen carrier for chemical looping with oxygen uncoupling process. Energy Fuels 2016;30(7):5953–63.
[9] Adánez-Rubio I, Bautista H, Izquierdo MT, Gayán P, Abad A, Adánez J. Development of a magnetic Cu-based oxygen carrier for the chemical looping with oxygen uncoupling (CLOU) process. Fuel Process Technol 2021;218:106836.
[10] Adánez-Rubio I, Samprón I, Izquierdo MT, Abad A, Gayán P, Adánez J. Coal and biomass combustion with CO_2 capture by CLOU process using a magnetic Fe-Mn-supported CuO oxygen carrier. Fuel 2022;314:122742.
[11] Schmitz M, Linderholm CJ. Performance of calcium manganate as oxygen carrier in chemical looping combustion of biochar in a 10 kW pilot. Appl Energy 2016;169:729–37.
[12] Moldenhauer P, Hallberg P, Biermann M, Snijkers F, Albertsen K, Mattisson T, et al. Oxygen-carrier development of calcium manganite-based materials with perovskite structure for chemical-looping combustion of methane. Energ Technol 2020;8(6).
[13] Pachler RF, Penthor S, Mayer K, Hofbauer H. Investigation of the fate of nitrogen in chemical looping combustion of gaseous fuels using two different oxygen carriers. Energy 2020;195.
[14] Frick V, Rydén M, Leion H, Mattisson T, Lyngfelt A. Screening of supported and unsupported Mn-Si oxygen carriers for CLOU (chemical-looping with oxygen uncoupling). Energy 2015;93:544–54.
[15] Pishahang M, Larring Y, Sunding M, Jacobs M, Snijkers F. Performance of perovskite-type oxides as oxygen-carrier materials for chemical looping combustion in the presence of H2S. Energ Technol 2016;4(10):1305–16.
[16] Schmitz M, Linderholm C, Lyngfelt A. Chemical Looping combustion of sulphurous solid fuels using spray-dried calcium manganate particles as oxygen carrier. Energy Procedia 2014;63:140–52.
[17] Shulman A, Cleverstam E, Mattisson T, Lyngfelt A. Manganese/iron, manganese/nickel, and manganese/silicon oxides used in chemical-looping with oxygen uncoupling (CLOU) for combustion of methane. Energy Fuels 2009;23(10):5269–75.
[18] Mattisson T, Jing D, Lyngfelt A, Rydén M. Experimental investigation of binary and ternary combined manganese oxides for chemical-looping with oxygen uncoupling (CLOU). Fuel 2016;164:228–36.
[19] Zhao H, Tian X, Ma J, Su M, Wang B, Mei D. Development of tailor-made oxygen carriers and reactors for chemical looping processes at Huazhong University of Science & Technology. Int J Greenhouse Gas Control 2020;93.
[20] Adánez J, Abad A, Mendiara T, Gayán P, de Diego LF, García-Labiano F. Chemical looping combustion of solid fuels. Prog Energy Combust Sci 2018;65:6–66.
[21] Lyngfelt A, Brink A, Langørgen Ø, Mattisson T, Rydén M, Linderholm C. 11,000 h of chemical-looping combustion operation—Where are we and where do we want to go? Int J Greenhouse Gas Control 2019;88:38–56.
[22] Mattisson T, Leion H, Lyngfelt A. Chemical-looping with oxygen uncoupling using CuO/ZrO_2 with petroleum coke. Fuel 2009;88(4):683–90.
[23] Mattisson T, Lyngfelt A, Leion H. Chemical-looping with oxygen uncoupling for combustion of solid fuels. Int J Greenhouse Gas Control 2009;3(1):11–9.

[24] Rydén M, Lyngfelt A, Mattisson T. Combined manganese/iron oxides as oxygen carrier for chemical looping combustion with oxygen uncoupling (CLOU) in a circulating fluidized bed reactor system. 4. 2011:341-8.
[25] Linderholm C, Mattisson T, Lyngfelt A. Long-term integrity testing of spray-dried particles in a 10-kW chemical-looping combustor using natural gas as fuel. Fuel 2009;88(11):2083–96.
[26] SUCCESS. Publishable Summary Report. EU 7th Framework Programme Collaborative Project; 2017.
[27] Oliveira VAG, Brett NH. Phase equilibria in the system MgO-Mn_2O_3-MnO-$CaSiO_3$ in air. Journal de Physique (Paris), Colloque 1986;47:453–9.
[28] Valverde-Diez N, Grande-Fernández D. Ternary compounds of the system Mg-Mn-O as oxygen sensors. Solid State Ionics 1988;28-30(PART 2):1697-700.
[29] Shulman A, Cleverstam E, Mattisson T, Lyngfelt A. Chemical – Looping with oxygen uncoupling using Mn/Mg-based oxygen carriers – Oxygen release and reactivity with methane. Fuel 2011;90(3):941–50.
[30] Hwang JH, Baek JI, Ryu HJ, Sohn JM, Lee KT. Development of $MgMnO_3.\delta$ as an oxygen carrier material for chemical looping combustion. Fuel 2018;231:290–6.
[31] Rydén M, Leion H, Mattisson T, Lyngfelt A. Combined oxides as oxygen-carrier material for chemical-looping with oxygen uncoupling. Appl Energy 2014;113:1924–32.
[32] Jing D, Jacobs M, Hallberg P, Lyngfelt A, Mattisson T. Development of $CaMn_{0.775}Mg_{0.1}Ti_{0.125}O_{3-\delta}$ oxygen carriers produced from different Mn and Ti sources. Mater Des 2016;89:527–42.
[33] ASTM. Standard test method for determination of attrition of FCC catalyst by air jets. ASTM D5757-11. Standard test method for determination of attrition of FCC catalyst by air jets 2006.
[34] Cabello A, Gayán P, García-Labiano F, de Diego LF, Abad A, Adánez J. On the attrition evaluation of oxygen carriers in Chemical Looping Combustion. Fuel Process Technol 2016;148:188–97.
[35] Adánez J, de Diego LF, García-Labiano F, Gayán P, Abad A, Palacios JM. Selection of oxygen carriers for chemical-looping combustion. Energy Fuels 2004;18(2):371–7.
[36] Adánez-Rubio I, Gayán P, Abad A, de Diego LF, García-Labiano F, Adánez J. Evaluation of a spray-dried CuO/$MgAl_2O_4$ oxygen carrier for the chemical looping with oxygen uncoupling process. Energy Fuels 2012;26(5):3069–81.
[37] Adánez-Rubio I, Nilsson A, Izquierdo MT, Mendiara T, Abad A, Adánez J. Cu-Mn oxygen carrier with improved mechanical resistance: Analyzing performance under CLC and CLOU environments. Fuel Process Technol 2021;217.
[38] Adánez-Rubio I, Izquierdo MT, Abad A, Gayan P, de Diego LF, Adánez J. Spray granulated Cu-Mn oxygen carrier for chemical looping with oxygen uncoupling (CLOU) process. Int J Greenhouse Gas Control 2017;65:76–85.
[39] Adánez-Rubio I, Arjmand M, Leion H, Gayán P, Abad A, Mattisson T, et al. Investigation of combined supports for cu-based oxygen carriers for chemical-looping with oxygen uncoupling (CLOU). Energy Fuels 2013;27(7):3918–27.
[40] Gayán P, Adánez-Rubio I, Abad A, de Diego LF, García Labiano F, Adánez J. Development of Cu-based oxygen carriers for Chemical-Looping with Oxygen Uncoupling (CLOU) process. Fuel 2012;96:226–38.